Int. J. Therm. Sci. (2000) 39, 130–139

S1290-0729(00)00198-7/FLA

Analysis of heat and mass transfer in asymmetric system

Kamar Boukrani [a], Claude Carlier [a], Alfred Gonzalez [a]*, Pierre Suzanne [b]

[a] *Laboratoire de Physique Appliquée et d'Automatique, Université de Perpignan 52, Avenue de Villeneuve 66860 Perpignan cedex, France*

[b] *Groupe Hauts Flux thermiques/DGA/DCE/CTA/LOT BP6, 66125 Font Romeu, France*

(Received 30 October 1998, accepted 14 May 1999)

Abstract — This study aims to investigate theoretically the effect of water evaporation from a wetted channel wall, on natural convection heat transfer and the effect of channel width. Major nondimensional groups identified are Gr_T, Gr_M, Pr, Sc and ϕ. Results are presented for an air–water system under various heating conditions. The influence of heated wall temperatures, wetted wall temperatures, channel width and the relative humidity of the moist air in the ambient on the heat and mass transfer are examined in great detail. © 2000 Éditions scientifiques et médicales Elsevier SAS

coupled transfer / natural convection / evaporation / vertical surface / asymmetric system

Nomenclature

b	channel width	m
Cp	specific heat	$W{\cdot}m^{-1}{\cdot}K^{-1}$
D	diffusion coefficient for water vapour	$m^2{\cdot}s^{-1}$
g	gravitational acceleration	$m{\cdot}s^{-2}$
Gr_T	Grashof number (heat transfer)	
Gr_M	Grashof number (mass transfer)	
l	channel length	m
M	molecular weight	$kg{\cdot}mol^{-1}$
Nu	Nusselt number	
p	pressure of the moist air in the channel	Pa
P	dimensionless motion pressure	
p_m	motion pressure (pressure deffect), $p - p_0$	Pa
p_0	ambient pressure	Pa
Pr	Prandtl number	
q	flow rate	$m^2{\cdot}s^{-1}$
Q	dimensionless flow rate	
Q_h	$(1/Sc)[(Cp_v - Cp_a)/Cp](w_r - w_0)$	
Sc	Schmidt number	
Sh	Sherwood number	
T	temperature	K
u	axial velocity	$m{\cdot}s^{-1}$
U	dimensionless axial velocity	
u_0	average inlet velocity	$m{\cdot}s^{-1}$
U_0	dimensionless average inlet velocity	
v	transverse velocity	$m{\cdot}s^{-1}$
V	dimensionless transverse velocity	
w	mass fraction of water vapour	$kg{\cdot}kg^{-1}$
W	dimensionless mass fraction of water vapour	
w_r	saturated mass fraction of water vapour at T_p and p_0	$kg{\cdot}kg^{-1}$
x	axial coordinate	m
X	dimensionless axial coordinate	
y	transverse coordinate	m
Y	dimensionless transverse coordinate	

Greek symbols

ρ	density	$kg{\cdot}m^{-3}$
μ	dynamic viscosity	$kg{\cdot}m^{-1}{\cdot}s^{-1}$
ν	kinematic viscosity	$m^2{\cdot}s^{-1}$
λ	thermal conductivity	$W{\cdot}m^{-2}{\cdot}K^{-1}$
ϕ	relative humidity of air at ambient condition	%

Subscripts

a	of air
p	condition at wetted wall (left channel wall)
0	at inlet condition
s	condition at the dry wall (right channel wall)
v	of water vapour

* Correspondence and reprints.
gonzalez@univ-perp.fr

1. INTRODUCTION

Situations often arise in which the combined buoyancy forces of thermal and mass diffusion resulting from the simultaneous presence of differences in temperature and variations in concentration have rather significant influences on heat transfer of flowing gas mixtures in engineering systems and the natural environment. In human bodies the simultaneous diffusion of metabolic heat and perspiration control our body temperature especially on hot summer days, the cooling of a high temperature surface by coating it with phase-change material and the process of evaporative cooling for waste heat disposal.

The natural convection heat transfer in vertical open channel flows induced by the buoyancy force of thermal diffusion alone has been studied in great detail [1–3].

The effects of the mass diffusion on laminar natural convection flows have been widely studied for flows over single plate with different conditions [4, 5] and for flows over vertical cylinder [6]. But in these studies, a very low concentration level was assumed such that the wall interfacial velocity can be neglected.

Despite natural convection due to the combined buoyancy forces of heat and mass diffusion between vertical parallel plates is relatively important in the application encountered in the engineering systems; and not received enough attention. Consideration is given, in the present study, to examining effects of wetted wall on natural convection heat transfer between vertical parallel plates and effects of channel width.

2. ANALYSIS

The geometry of the system to be examined as schematically shown in *figure 1*, is an open-ended vertical parallel plates with length l and channel width b. The left channel wall is wetted by a thin water film. As a preliminary attempt, the film is assumed to be extremely thin so that it can be regarded as a boundary condition for heat and mass transfer; the film is therefore considered stationary and at the same uniform temperature as the wall, T_p. The right channel wall is kept at the constant and uniform temperature, T_s.

The moist air in the ambient space is drawn into the channel by the simultaneous action of combined buoyancy forces resulting from the nonuniformities in temperature and in concentration of water vapour in the flow between the channel plates and the outer space.

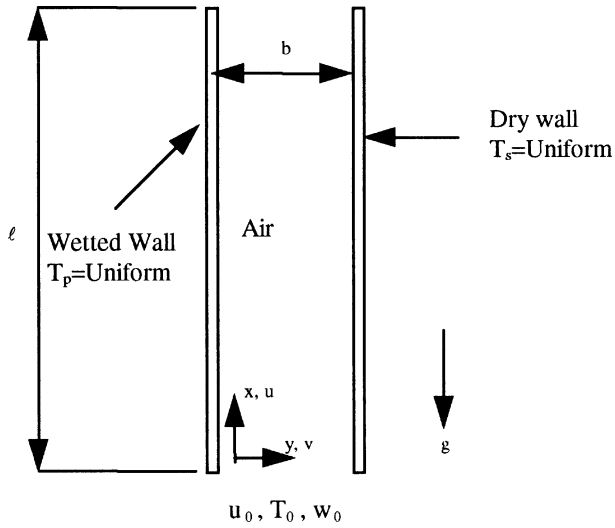

Figure 1. Schematic diagram of the physical system.

Since the molecular weight of water vapour is smaller than that of air, the buoyancy force due to mass transfer acts upward. As a result, the flow induced by the buoyancy force of heat transfer if $T_p > T_0$ while the flow is retarded if $T_p < T_0$.

2.1. Governing equations

In the present study the following major simplifying assumptions are made:

(1) The flow is laminar and steady.

(2) All physical properties of the fluid are constant except for the density in the buoyancy term.

(3) Boundary-layer approximations are valid. This is justified, provided the channel length–width ratio is much larger than unity [7].

(4) Viscous dissipation and pressure work are negligible.

(5) Secondary phenomena of thermal diffusion and diffusion thermal effects are neglected.

(6) Radiation effect between the channel walls can be neglected.

In assumption (6), we have neglected the thermal radiation effect. This assumption is reasonable because the main of this work is to investigate the role of latent heat transfer played in the combined heat and mass transfer in natural convection.

With the above assumptions, the steady natural convection flow of a gas mixture in a vertical channel re-

sulting from the combined buoyancy effects of heat and mass diffusion can be described by the basic equations in nondimensionless form as

- *Continuity equation*:

$$\frac{\partial u}{\partial x} + \frac{\partial v}{\partial y} = 0 \tag{1}$$

- *Axial-momentum equation*:

$$u\frac{\partial u}{\partial x} + v\frac{\partial u}{\partial y} = -\frac{1}{\rho}\frac{\partial p_{\mathrm{m}}}{\partial x} + g\left(\frac{(T-T_0)}{T_0} + \left(\frac{M_{\mathrm{a}}}{M_{\mathrm{v}}} - 1\right)(w - w_0)\right) + v\frac{\partial^2 u}{\partial y^2} \tag{2}$$

In writing this equation, we have introduced the concept of pressure defect or motion pressure, p_{m}, which is the imbalance between the pressure within the channel and that in the ambient space. Moreover, the boundary-layer approximations have been made. The third term on the right-hand side is the buoyancy forces induced by thermal and mass diffusion.

- *Energy equation*:

$$u\frac{\partial T}{\partial x} + v\frac{\partial T}{\partial y} = \frac{\lambda}{\rho\, Cp}\frac{\partial^2 T}{\partial y^2} + D\frac{(Cp_{\mathrm{v}} - Cp_{\mathrm{a}})}{Cp}\frac{\partial T}{\partial y}\frac{\partial w}{\partial y} \tag{3}$$

The last term on the right-hand side of this equation represents the energy transport through the interdiffusion of the species, air and water vapour.

- *Concentration equation*:

$$u\frac{\partial w}{\partial x} + v\frac{\partial w}{\partial y} = D\frac{\partial^2 w}{\partial y^2} \tag{4}$$

- *Flow rate equation*:

$$q = \int_0^{\mathrm{b}} u(x, y)\,\mathrm{d}y \tag{5}$$

3. MAIN EQUATIONS SYSTEM

By making use of the equation of state for ideal gas mixture and assuming low level of water vapour concentration, the density variation in the moist air can be approximated by

$$\frac{\rho_0 - \rho}{\rho} = \frac{1}{T_0}(T - T_0) + \left(\frac{M_{\mathrm{a}}}{M_{\mathrm{v}}} - 1\right)(w - w_0) \tag{6}$$

where M_{a} and M_{v} are the molecular weights of air and water vapour, respectively.

Assuming that the air–water interface is semi-permeable (that is, the solubility of air in water is negligibly small and air is stationary at the interface), the velocity of mixture on the wetted wall can be evaluated by [8]

$$v_{\mathrm{p}} = -\frac{D}{1 - w_{\mathrm{p}}}\left.\frac{\partial w}{\partial y}\right|_{y=0} \tag{7}$$

According to Dalton's law and the equation of state for the ideal gas mixture, the interfacial mass fraction of water vapour can be calculated by the equation

$$w_{\mathrm{p}} = \frac{p_{\mathrm{p}} M_{\mathrm{v}}}{p_{\mathrm{p}} M_{\mathrm{v}} + (p - p_{\mathrm{p}}) M_{\mathrm{a}}} \tag{8}$$

where p_{p} is the partial pressure of water vapour at interface.

It is worth noting that the pressure p varies with x, so does w_{p}. This prohibits us from taking w_{p} as a reference scale in the nondimensionalization process. Instead, w_{r} is employed, which is the saturated mass fraction of water vapour at T_{p} and p_0 [9]:

$$w_{\mathrm{r}} = \frac{0.622 f_{\mathrm{p}}}{P - 0.378 f_{\mathrm{p}}} \tag{9}$$

with $f_{\mathrm{p}} = 10^{17.443 - 2795/T_{\mathrm{p}} - 3.868 \log T_{\mathrm{p}}}$.

In this study, the thermophysical properties of the mixture are taken to be constant and are evaluated by one-third rule. The complete details on the evaluation of properties of air, water vapour and their mixture are available in [10].

Equations (1)–(4) are subjected to the following boundary conditions:

$$\begin{aligned}
&u(0, y) = u_0, && T(0, y) = T_0\\
&w(0, y) = w_0, && p(0, y) = -\frac{\rho_0 u_0^2}{2}\\
&u(x, 0) = 0, && T(x, 0) = T_{\mathrm{p}}\\
&w(x, 0) = w_{\mathrm{p}}(x), && v(x, 0) = v_{\mathrm{p}}(x)\\
&u(x, b) = 0, && v(x, b) = 0\\
&\left.\frac{\partial w}{\partial y}\right|_{y=b} = 0, && p_{\mathrm{m}}(l, y) = 0
\end{aligned} \tag{10}$$

4. ADIMENSIONALIZATION METHOD

The following dimensionless variables are introduced:

$$
\begin{aligned}
&X = \frac{x}{l(Gr_{\mathrm{Tr}} + Gr_{\mathrm{Mr}})}, \qquad && Y = \frac{y}{b} \\
&W = \frac{w - w_0}{w_{\mathrm{r}} - w_0}, && \theta = \frac{T - T_0}{T_{\mathrm{p}} - T_0} \\
&U = \frac{ub^2}{l\nu(Gr_{\mathrm{Tr}} + Gr_{\mathrm{Mr}})}, && V = \frac{vb}{\nu} \\
&P = \frac{p_{\mathrm{m}} b^4}{\rho l^2 \nu^2 (Gr_{\mathrm{Tr}} + Gr_{\mathrm{Mr}})^2} \\
&Gr_{\mathrm{T}} = \frac{g(T_{\mathrm{p}} - T_0)b^4}{l\nu^2 T_0} \\
&Gr_{\mathrm{M}} = g\left(\frac{M_{\mathrm{a}}}{M_{\mathrm{v}}} - 1\right)\frac{(w_{\mathrm{p}} - w_0)b^4}{l\nu^2} \\
&Pr = \frac{\mu\, Cp}{\lambda}, && Sc = \frac{\nu}{D} \\
&Q_{\mathrm{h}} = \frac{1}{Sc}\,\frac{Cp_{\mathrm{v}} - Cp_{\mathrm{a}}}{Cp}\,(w_{\mathrm{r}} - w_0)
\end{aligned}
\tag{11}
$$

Note that Gr_{Tr} and Gr_{Mr} are respectively the Grashof numbers for heat and mass transfer at the reference condition:

$$
T_{\mathrm{ref}} = T_{\mathrm{p}} - \frac{T_{\mathrm{p}} - T_0}{3} \qquad w_{\mathrm{ref}} = w_{\mathrm{p}} - \frac{w_{\mathrm{p}} - w_0}{3}
$$

The use of Gr_{Tr} and Gr_{Mr} leads to a physically more meaningful comparison among various cases studied.

The governing equations then become:

- *Continuity equation*:

$$
\frac{\partial U}{\partial X} + \frac{\partial V}{\partial Y} = 0 \tag{12}
$$

- *Axial-momentum equation*:

$$
U\frac{\partial U}{\partial X} + V\frac{\partial U}{\partial Y} = -\frac{\mathrm{d}P}{\mathrm{d}X} + \frac{\partial^2 U}{\partial Y^2} + \frac{Gr_{\mathrm{T}}\theta + Gr_{\mathrm{M}}W}{Gr_{\mathrm{Tr}} + Gr_{\mathrm{Mr}}} \tag{13}
$$

- *Energy equation*:

$$
U\frac{\partial \theta}{\partial X} + V\frac{\partial \theta}{\partial Y} = \frac{1}{Pr}\frac{\partial^2 \theta}{\partial Y^2} + Q_{\mathrm{h}}\frac{\partial \theta}{\partial Y}\frac{\partial W}{\partial Y} \tag{14}
$$

- *Concentration equation*:

$$
U\frac{\partial W}{\partial X} + V\frac{\partial W}{\partial Y} = \frac{1}{Sc}\frac{\partial^2 W}{\partial Y^2} \tag{15}
$$

- *Flow rate equation*:

$$
Q = \int_0^1 U(X, Y)\,\mathrm{d}Y \tag{16}
$$

- *Boundary conditions*. The dimensionless boundary conditions become

$$
\begin{aligned}
&U(0, Y) = U_0, && \theta(0, Y) = 0 \\
&W(0, Y) = 0, && P(0, Y) = -\frac{U_0^2}{2} \\
&U(X, 0) = 0, && V(X, 0) = V_{\mathrm{p}}(X) \\
&\theta(X, 0) = 1, && W(X, 0) = \frac{w_{\mathrm{p}}(x) - w_0}{w_{\mathrm{r}} - w_0} \\
&U(X, 1) = 0, && \left.\frac{\partial W}{\partial Y}\right|_{Y=1} = 0 \\
&P\left(\frac{1}{Gr_{\mathrm{Tr}} + Gr_{\mathrm{Mr}}}\right) = 0
\end{aligned}
\tag{17}
$$

with

$$
V_{\mathrm{p}}(X) = -\frac{1}{Sc}\,\frac{w_{\mathrm{r}} - w_0}{1 - w_{\mathrm{p}}(x)}\left.\frac{\partial W}{\partial Y}\right|_{Y=1}
$$

It should be noted that both magnitude and shape of the inlet velocity U_0 are not known before the complete solution for the governing equations, including the entrance and end effects, is obtained.

In many investigations [11, 12], it was shown that magnitude of U_0 can be determined from the solution processes, and that the shape of U_0 has little effect on heat and mass transfer in the flow. Thus, in the present study U_0 is assumed to be uniform, and its magnitude will be found by the iterative procedures in the numerical solution.

Energy transport from the wetted wall to moist air in the presence of mass transfer depends on two related factors [13]:

– the fluid temperature gradient at the wetted wall,

– the mass transfer rate.

A local Nusselt number is defined as

$$
\begin{aligned}
Nu_x &= -\frac{(\partial T/\partial y)_{y=0}\, x}{T_{\mathrm{s}} - T_0} \\
&= -\frac{(\partial \theta/\partial Y)_{Y=0}\, X(Gr_{\mathrm{T}} + Gr_{\mathrm{M}})l}{b}
\end{aligned}
\tag{18}
$$

Similarly, the local Sherwood number on the wetted wall can be defined as

$$
\begin{aligned}
Sh_x &= -\frac{(\partial w/\partial y)_{y=0}\, x}{w_{\mathrm{s}} - w_0} \\
&= -\frac{(\partial W/\partial Y)_{Y=0}\, X(Gr_{\mathrm{T}} + Gr_{\mathrm{M}})l}{b}
\end{aligned}
\tag{19}
$$

5. SOLUTION METHOD

Because flow under consideration is of the boundary layer type, the solution for equations (12)–(16) can be marched in the downstream direction. A fully implicit numerical scheme in which the axial convection is approximated by the upstream difference, the transverse convection and diffusional terms by the central difference, is employed to transform the governing equations into finite-difference equations [14]. We obtain a set of matrices, for which an inverse method to obtain the numerical solution can be used.

To approximate the equation (13) by the finite-difference numerical method, we have introduced the notation $U(i, j)$ corresponding to the point $(i\Delta X, j\Delta Y)$ after discretization according to OX and OY. The same notation is used for other functions V, P, θ and W with

$$0 \le X \le \frac{1}{Gr_{\mathrm{Tr}} + Gr_{\mathrm{Mr}}}, \qquad 0 \le Y \le 1$$

5.1. System of axial-momentum equations

$$\begin{aligned}
&\left(\frac{U(i,j)}{\Delta X} + \frac{2}{(\Delta Y)^2}\right) U(i+1,j) \\
&\quad = \left(\frac{1}{(\Delta Y)^2} - \frac{V(i,j)}{2\Delta Y}\right) U(i+1,j+1) \\
&\qquad + \left(\frac{V(i,j)}{2\Delta Y} + \frac{1}{(\Delta Y)^2}\right) U(i+1,j-1) \\
&\qquad + \frac{U(i,j)U(i,j)}{\Delta X} \\
&\qquad + \frac{Gr_{\mathrm{T}}\theta(i,j) + Gr_{\mathrm{M}} W(i,j)}{Gr_{\mathrm{Tr}} + Gr_{\mathrm{Mr}}} \\
&\qquad - \frac{P(i+1,j) - P(i,j)}{\Delta X} \\
&U(i+1,0) = U(i+1,JJ) = 0
\end{aligned} \tag{20}$$

with $0 \le i \le II-1$, $1 \le j \le JJ-1$ for some II and JJ.

We complete this system by the following equation:

$$Q = \sum_{j=1}^{JJ-1} U(i,j)\Delta Y \tag{21}$$

5.2. System of energy equations

$$\begin{aligned}
&\left(\frac{U(i+1,j)}{\Delta X} + \frac{2}{Pr(\Delta Y)^2}\right)\theta(i+1,j) \\
&\quad = \left(-\frac{V(i,j)}{2\Delta Y} + \frac{1}{Pr(\Delta Y)^2} + \frac{Q_{\mathrm{h}}}{4(\Delta Y)^2}\right. \\
&\qquad \left.\cdot \big(W(i+1,j+1) - W(i+1,j-1)\big)\right) \\
&\qquad \cdot \theta(i+1,j+1) \\
&\qquad + \left(\frac{V(i,j)}{2\Delta Y} + \frac{1}{Pr(\Delta Y)^2} - \frac{Q_{\mathrm{h}}}{4(\Delta Y)^2}\right. \\
&\qquad \left.\cdot \big(W(i+1,j+1) - W(i+1,j-1)\big)\right) \\
&\qquad \cdot \theta(i+1,j-1) + \frac{U(i,j)}{\Delta X}\theta(i,j) \\
&\theta(i+1,0) = 1, \qquad \theta(i+1,JJ) = \frac{T_{\mathrm{s}} - T_0}{T_{\mathrm{p}} - T_0}
\end{aligned} \tag{22}$$

with $0 \le i \le II-1$, $1 \le j \le JJ-1$.

5.3. System of concentration equation

$$\begin{aligned}
&\left(\frac{U(i+1,j)}{\Delta X} + \frac{2}{Sc(\Delta Y)^2}\right) W(i+1,j) \\
&\quad = \left(\frac{1}{Sc(\Delta Y)^2} - \frac{V(i,j)}{2\Delta Y}\right) W(i+1,j+1) \\
&\qquad + \left(\frac{V(i,j)}{2\Delta Y} + \frac{1}{Sc(\Delta Y)^2}\right) W(i+1,j-1) \\
&\qquad + \frac{U(i+1,j)}{\Delta X} W(i,j) \\
&W(i+1,0) = 1, \qquad W(i+1,JJ-1) = W(i+1,JJ)
\end{aligned} \tag{23}$$

with $0 \le i \le II-1$, $1 \le j \le JJ-1$.

5.4. Algorithm

The guessed value of inlet velocity U_0 influences the speed and the convergence of the algorithm. Its exact value is only known at the end of calculations, also we have take a value given in the literature for a system presenting a significant l/b ratio and which be a reasonable initial value for the study system [7].

A brief outline of the solution procedures is described as follows:

Step 1. Guess an inlet velocity U_0.

Step 2. For any axial location, solve the system of equations (12)–(16) for U, P, θ and W.

Step 3. Integrate the continuity equation numerically to find V:

$$V = -\frac{\partial}{\partial X}\int_0^Y U\,\mathrm{d}Y \tag{24}$$

Step 4. If the total mean-square errors for the velocity, temperature and concentration between two consecutive iterations satisfy the criterion [14]

$$\sum_{j=1}^{JJ}\left[\left(U_{i,j}^{n}-U_{i,j}^{n-1}\right)^2+\left(W_{i,j}^{n}-W_{i,j}^{n-1}\right)^2 + \left(Q_{i,j}^{n}-Q_{i,j}^{n-1}\right)^2\right] < 10^{-6}, \quad 1 \le i \le II \tag{25}$$

then the solution for the current axial location is complete. Now if equation (25) is not met, go to step 2 and solve finite-difference equations for U, θ and W and use equation (24) to get V until the condition specified in equation (25) is fulfilled.

Step 5. Procedures (2)–(4) are successively applied to every axial location from the channel entrance to the exit of channel.

Step 6. Check whether the exit pressure is $P = 0$. If not, go to step 1, guess a new inlet velocity U_0 by Newton–Raphson method [13] and proceed the procedures (2)–(6). If yes, the solution is completed.

To obtain enhanced accuracy in the numerical computation, grids are chosen to be uniform in the Y direction which is believed to be appropriate in the assumption of laminar flows, while in the X direction a nonuniform grid is employed to account for the drastic variations of velocity, temperature and concentration in the near-entrance region.

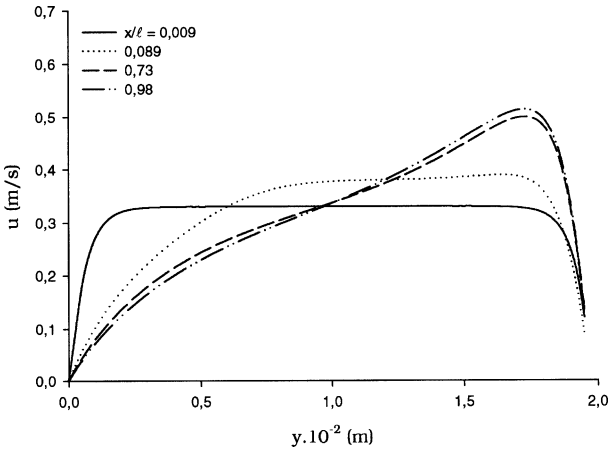

(*a*)

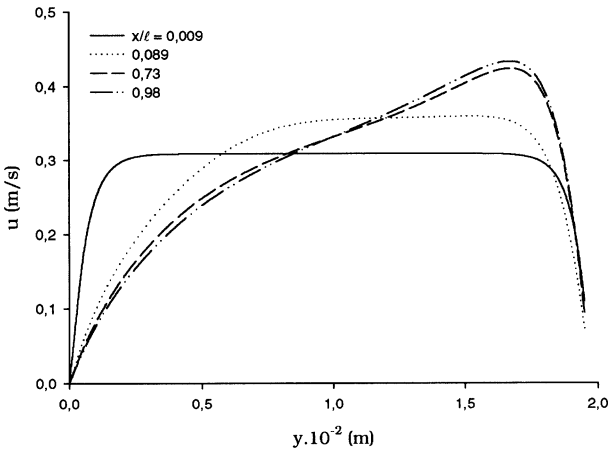

(*b*)

Figure 2. Developments of axial velocity profiles. (*a*) T_p = 309 K, T_s = 339 K, l = 0.5 m, b = 0.02 m, ϕ = 50 %. (*b*) T_p = 309 K, T_s = 320 K, l = 0.5 m, b = 0.02 m, ϕ = 50 %.

6. RESULTS AND DISCUSSION

In the present study, the calculations are performed for air–water vapour mixture flowing in the narrow channel, a situation widely found in engineering systems. Other mixtures can be solved in the same way.

It should be emphasized that not all the values for the nondimensional groups, i.e. Pr, Sc, Gr_T, Gr_M, etc., can be arbitrarily assigned. In fact, they are interdependent for a given mixture under specific conditions. In the light of practical situations, T_0, T_p, T_s, ϕ and l are chosen as the independent parameters. All the nondimensional parameters can then be evaluated.

All the cases studied in this work are based on a finite vertical open channel with length of 0.5 m.

The results are presented in dimensional form to have a precise idea about size of different parameters studied. The curves of the various figures are plotted for differents positions in the channel characterized by the report x/l.

Shown in *figure 2* are the developments of the axial velocity in the channel under various conditions. It is clearly seen that the velocity profiles develop gradually from the uniform distributions to the distorted ones, a situation normally found in laminar channel flows without mass addition. But the mass flow rate keeps increasing as the air moves downstream due to the

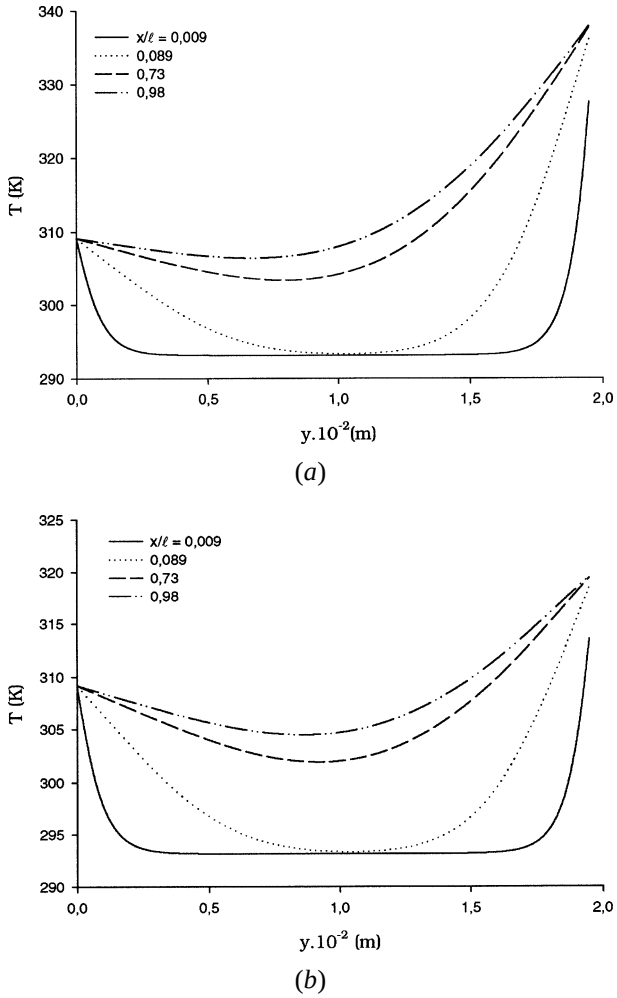

Figure 3. Developments of temperature profiles. (*a*) $T_p = 309$ K, $T_s = 339$ K, $l = 0.5$ m, $b = 0.02$ m, $\phi = 50$ %. (*b*) $T_p = 309$ K, $T_s = 320$ K, $l = 0.5$ m, $b = 0.02$ m, $\phi = 50$ %.

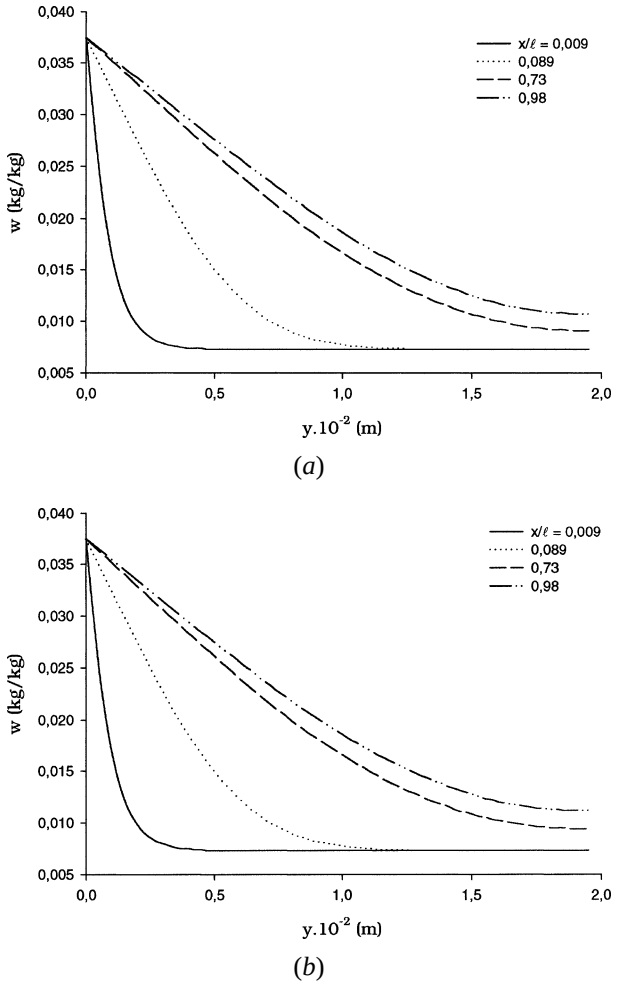

Figure 4. Developments of mass-fraction profiles. (*a*) $T_p = 309$ K, $T_s = 339$ K, $l = 0.5$ m, $b = 0.02$ m, $\phi = 50$ %. (*b*) $T_p = 309$ K, $T_s = 320$ K, $l = 0.5$ m, $b = 0.02$ m, $\phi = 50$ %.

evaporation of water vapour into the air stream from the water film on the left channel wall.

In *figure 2a* the fluid near the right wall is accelerated to a higher speed due to T_s being much higher than T_p.

Comparing *figure 2a* and *figure 2b* indicates that an increase in T_s results in an increase in axial velocity u, in conformity with a larger buoyancy force through thermal and mass diffusion.

The developments of temperature, T, and mass fraction of water vapour, w, are plotted in *figures 3* and *4*, respectively.

In *figure 3*, it is seen that the temperature profiles pass through a minimum to draw nears the ambient temperature.

In *figure 4*, it is clear that in line with the evaporation of water vapor from the wetted wall into the air stream, the mass fraction of water vapour increases gradually as the air goes downstream.

Normally, the mass fraction of water vapor on the wetted surface, for difference gradients of temperature, is a function of pressure gradient, therefore function of the position according to ox. In the studied system, because of the small pressure defect in the flow, this mass fraction is constant and equal to that obtained in the event of saturation w_r.

To illustrate the effect of channel width, the temperature profiles for various widths are shown in *figure 5*. The comparison of two simulations makes it possible to conclude that the convection is started only if the thick-

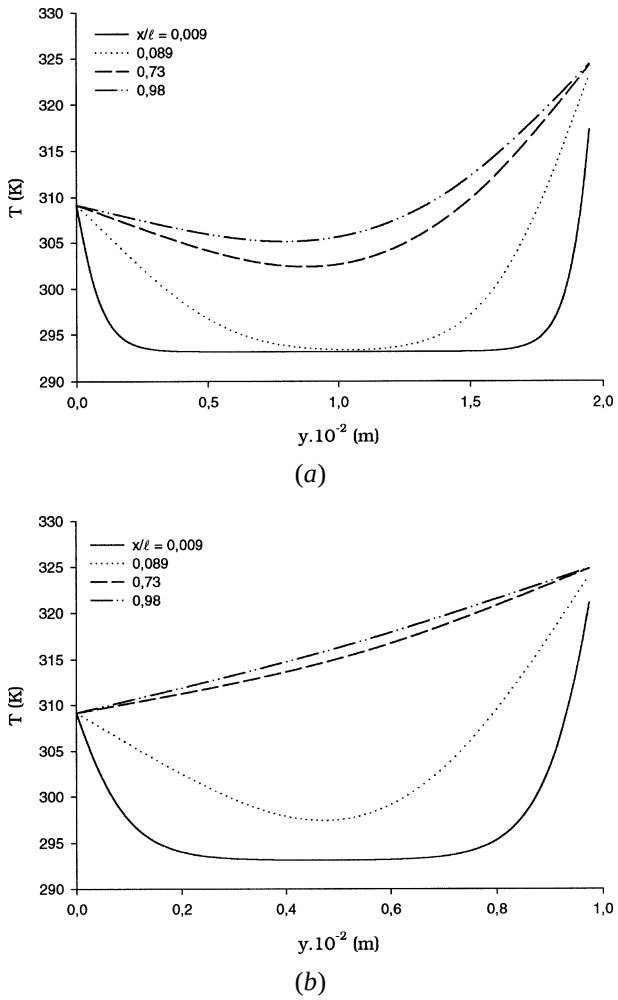

Figure 5. Developments of temperature profiles. (*a*) $T_p = 309$ K, $T_s = 325$ K, $l = 0.5$ m, $\phi = 50$ %, $b = 0.02$ m. (*b*) $T_p = 309$ K, $T_s = 325$ K, $l = 0.5$ m, $\phi = 50$ %, $b = 0.01$ m.

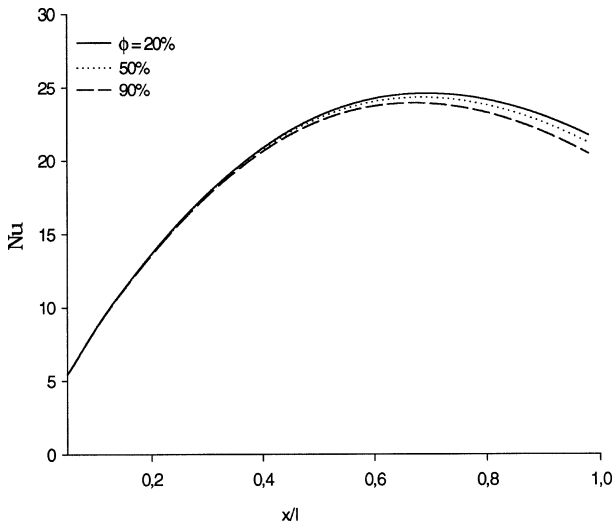

Figure 6. Local Nusselt number at different ambient humidity. $T_p = 309$ K, $T_s = 325$ K, $l = 0.5$ m, $\phi = 50$ %, $b = 0.02$ m.

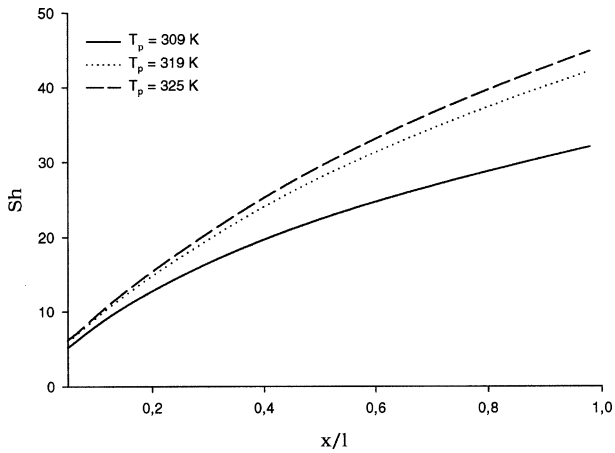

Figure 7. Local Sherwood number along the wetted wall at different temperature of the wetted wall. $T_s = 339$ K, $l = 0.5$ m, $b = 0.02$ m, $\phi = 50$ %.

ness is sufficient. If b is equal to 10^{-2} m, the heat transfer is done only by conduction. The profile is linear. If b is greater than 10^{-2} m, the convection is set in motion. This leads a cooling of air. In this case, the temperature profiles pass through a minimum to draw near the ambient temperature.

It is interesting to examine the effect of the ambient relative humidity on the transport of latent heat. Depicted in *figure 6* is the local Nusselt number Nu_x along the wetted wall.

Close inspection on *figure 6* discloses that better latent heat transport is noticed for the flow with a lower ambient humidity ϕ. This finding can be made plausible by recognising that the latent heat exchange connected with evaporation of the water film in the wetted film is very large, and thus a slight increase in the liquid evaporation by lowering ϕ can cause a substantial increase in the latent heat exchange.

The effect of wetted wall temperature on the heat transfer is illustrated in *figure 7*. A larger Sh_x is experienced for a larger temperature T_s. This phenomenon can be explained by the significant difference existing between the specific heats of the water vapor and of the dry air. In gas film formed in the vicinity of the wetted wall, the vapor leaving surface emmagazine calorific energy. The thermal balance with the surrounding air is es-

TABLE I
Values of major parameters for various cases.

T_s	T_p	Pr	Sc	Gr_T	Gr_M	Gr_{Tr}	Gr_{Mr}
339	309	0.69	0.55	675.07	226.85	450.04	151.23
339	319	0.69	0.55	1024.8	402.61	268.4	683.13
339	325	0.68	0.55	1214.3	548.71	365.81	809.51

tablished at a higher temperature. Consequently, the heat transfers by conduction between the heated surface and air decrease. So, this results from the higher latent heat transport in association with the larger water evaporation from the wetted wall. Results are obtained for several cases presented in *Table I*.

7. CONCLUSION

The nature of natural convection flows between vertical parallel plates resulting from the combined buoyancy effects of heat and mass diffusion has been studied, in particular for the air–water systems. The influence of the heated wall temperature, channel width and the relative humidity of the moist air in the ambient on heat and mass transfer in the flow are examined in great detail.

What follows is a brief summary of the major results:

– Heat transfer in the flow is dominated by the transport of latent heat in connection with the vaporisation of the water film on the wetted wall.

– The flow rate into the channel by the combined buoyancy forces of thermal and mass diffusion increases significantly with b, as the channel is wide. While for a narrow channel, the heat transfer occurs solely by conduction.

– An increase in relative humidity ϕ results in a slight decrease in Nusselt number.

Results presented above are based on a number of assumptions made in the study. To test the validity of the assumptions, further research must be pursued.

It is clear that when the system operates at high temperatures, the use of Boussinesq approximation is simply inappropriate. This becomes a serious problem especially for an air–water system for the reason that the water vapour contained in the mixture could be in significant amount when the mixture is at a higher temperature.

Additionally, it is also noted that when the system operates at large Grashof numbers, the flow field induced in the vertical channel would undergo transition from laminar to turbulent flow. Hence, the predicted results in the study become invalid. It is conceivable to study the combined heat and mass transfer in buoyancy driven flows with the simultaneous presence of laminar, transitional turbulent flow regimes and include the flow and thermal fields in the regions surrounding the tube ends.

The aim of our study is the establishment of the model in steady state intended for the analysis of coupled heat and mass transfers between the skin and fabric of protection. The second shutter of this article presents the comparison between the numerical simulations and the experimental results obtained by an inverse method based on holographic interferometry.

Acknowledgement

The support of this research by Groupe Hauts Flux thermiques/DGA/DCE/CTA/LOT., throught the contract 20496/97 is gratefully acknowledged.

REFERENCES

[1] Bodoia J.-R., Osterle J.-F., The development of free convection between heated vertical plates, J. Heat Transfer 84 (1962) 40–44.

[2] Writz R.-A., Stutzman R.-J., Experiments on free convection between vertical plates with symmetric heating, J. Heat Transfer 104 (1982) 501–507.

[3] Sabri A., Contribution à l'étude des transferts thermiques et massiques lors de la transpiration d'une plaque poreuse en convection naturelle, thèse, Université de Perpignan, 1996.

[4] Bottemanne F.-A., Theoretical solution of simultaneous heat and mass transfer by free convection about a vertical flat plate, Appl. Sci. Res. 25 (1971) 137–149.

[5] Chen T.-S., Yuh C.-F., Combined heat and mass transfer in natural convection along a vertical cylinder, Internat. J. Heat Mass Transfer 23 (1979) 451–461.

[6] Chang C.-J., Lin T.-F., Yan W.-M., Combined heat and mass transfer in natural convection between vertical parallel plates, Warme- und Stoffübertragung 23 (1988) 69–76.

[7] Chow L.-C., Chang C.-J., Evaporation of water into a laminar stream of air and superheated steam, Internat. J. Heat Mass Transfer 26 (1983) 373–380.

[8] Baumann W.-M., Thiele F., Heat and mass transfer in two-component film evaporation in a vertical tube, in: Proc. 8th Int. Heat Transfer, San Francisco 4, 1986, pp. 1843–1848.

[9] Chang C.-J., Lin T.-F., Yan W.-M., Natural convection flows in a vertical open tube resulting from combined buoyancy effects of thermal and mass diffusion, Internat. J. Heat Mass Transfer 29 (1986) 1543–1552.

[10] Fujji T., Kato Y., Mihara K., Expressions of transport and thermodynamics properties of air, steam and water, Report 66, Kyu Shu University, Japan, 1977.

[11] Eckert E.R.G., Drake R.-M., Analysis of Heat and Mass Transfer, McGraw-Hill, New York, 1972.

[12] Patankar S.V., Numerical Heat Transfer and Fluid Flow, McGraw-Hill, New York, 1980.

[13] Tannehill J.C., Anderson D.A., Pletcher R.H., Computational Fluid Mechanics and Heat Transfer, 2nd edition, Taylor & Francis, 1997.

[14] Nougier J.P., Méthodes de calcul numérique, 3^{e} édition, Masson, Paris, 1987.